On the internal kinematics of PNe

Ralf Jacob[1], Detlef Schönberner[1], Holger Lehmann[2], Alena Zwanzig[1], Christer Sandin[1] and Matthias Steffen[1]

[1]Leibniz-Institut für Astrophysik Potsdam,
An der Sternwarte 16, D–14482 Potsdam, Germany
email: `rjacob@aip.de`

[2]Thüringer Landessternwarte Tautenburg,
Sternwarte 5, D–07778 Tautenburg, Germany

Abstract. Our sample of round/elliptical double-shell PNe around central stars (CSs) with H-rich surface chemistry covers all evolutionary phases across the HRD. By means of high-resolution and high-S/N spectra we determine bulk matter velocities of the inner wind-driven rims and the maximum (= post-shock) gas velocities of the surrounding thermally expanding shells. Studying the details of the internal kinematics allows a look at processes of PN formation and at PN expansion history helping, for instance, to determine expansion distances.

Keywords. hydrodynamics, planetary nebulae: general, stars: AGB and post-AGB

We considerably extended our earlier study based on ESO-CAT/CES, NTT/EMMI, and NOT/IACUB spectra (Schönberner *et al.* 2005a) by additional data mostly gained from the Coudé-échelle spectrograph at the 2m-telescope at Tautenburg and, in parts, from ESO-VLT/FLAMES-ARGUS. We proceeded, as recommended by Corradi *et al.* (2007), with measuring the post-shock velocity, $V_{\rm shell}$, at the shell's leading edge from the outer peaks of the line profiles's 1st derivative. The bulk velocity of the rim, $V_{\rm rim}$, was determined by Gaussian fits (Fig. 1, top left). Our sample comprises now about 30 round/elliptical PNe from the Galactic disk & halo, and from the Sgr dwarf galaxy. Our study of Galactic disk PNe confirms our previous results based on a much smaller sample: both rim and shell accelerate with time/evolution, but such that their difference velocities, $(V_{\rm shell} - V_{\rm rim})$, remain roughly constant (Fig. 1, top right). This finding is at variance with the commonly used assumption that PNe expand homologously, but in agreement with the prediction of 1-dim radiation-hydrodynamics simulations if realistic initial conditions and time-evolution of stellar winds and radiation fields are considered: The shell's expansion starts well above a typical AGB-wind velocity of ca. $10 \ {\rm km \, s^{-1}}$, in line with the fact that ionization and heating occur in the so far undisturbed AGB wind. On the other side, the rim forms out of material which has already been decelerated below the original AGB-wind velocity by the high pressure of the ionized shell, and its evolution is virtually stalled at the outset.

We expect the expansion properties of PNe to depend on metallicity, Z: the power of line-driven winds decreases with Z due to reduced line opacities, yielding lower $V_{\rm rim}$. The shell dilutes faster because of the higher electron temperature, due to a reduced cooling efficiency at low Z (Schönberner *et al.* 2010, and refs. therein). We also successfully obtained spatially resolved spectrograms of four metal-poor PNe (Fig. 1, bottom right). The smaller number and the fact that their CS's effective temperatures are more uncertain hamper the comparison with the Galactic disk (GD) PNe. However, $V_{\rm rim}$ and $V_{\rm shell}$ of the low-Z PNe are clearly located at the lower and upper envelopes of the found correlations – in support of the theoretical arguments.
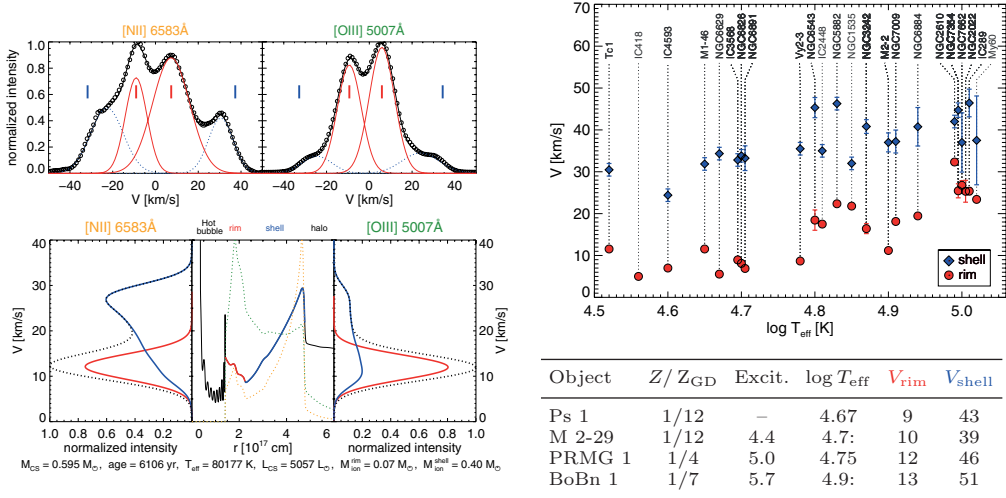
Figure 1. *Top left*: typical observed line-profile shapes (example NGC 6826) and their decomposition into four Gaussians for two prominent emission lines (black circles). The inner components represent the rim expansion (red solid) whereas the faster, but fainter wings trace the expansion of the shell (blue dotted). In [N II] the shell component is more pronounced due to still persisting ionization stratification in this middle-aged object. The black solid line gives the sum of the four Gaussians. The vertical bars indicate the velocities deduced for the corresponding components (red solid/blue solid). *Bottom left*: 1D-RHD simulation snapshot from a sequence around a CS of $M = 0.595 \, M_\odot$ at parameters listed in the panel. All three panels share the same y-axis. While the middle panel depicts the radial velocity structure, the outer panels show the approaching component of the corresponding (symmetric) central emission line profiles (black dotted) as well as the individual contributions of rim and shell. The middle panel also shows the ion density distributions of O^{2+} and N^+, resp., in arbitrary units (colored dotted lines). *Top right*: velocity components of rim & shell vs. CS temperatures as proxy for evolutionary state (from NLTE analysis or He II-Zanstra temperature) for our sample of Galactic disk PNe. *Bottom right*: expansion velocities in km s^{-1} for four metal-poor PNe observed with VLT/FLAMES together with nebular excitation class and CS effectice temperature. Metallicities (Howard *et al.* 1997) are given relative to mean Galactic disk composition (Schönberner *et al.* 2005a).

Throughout their entire life, PNe are, even in their simplest possible morphology, active dynamical systems with a velocity field whose shape changes considerably with time/evolution due to ever changing boundary conditions. First photoionization and later also wind interaction are the dominant physical processes in shaping round/elliptical PNe and in controlling their evolution. Note that any homologous expansion law, whether $\dot{R} \sim R$ or $V \sim R$, assumes implicitly a ballistic expansion from a common center. However, simulations show that the independently expanding rim and shell are formed by hydrodynamics at different times *and* at different distances from the star. Moreover, the boundaries of rim & shell are either shock or ionization fronts and their expansion cannot be measured spectroscopically. In order to obtain the real expansion, partly large corrections to the measured Doppler velocities have to be applied depending on structure and evolutionary state (Schönberner *et al.* 2005b).

References

Corradi, R. L. M., Steffen, M., Schönberner, D., & Jacob, R. 2007, *A&A*, 474, 529
Howard, J. W., Henry, R., & McCarthy, S. 1997, *MNRAS*, 284, 465
Schönberner, D., Jacob, R., Steffen, M., *et al.* 2005a, *A&A*, 431, 963
Schönberner, D., Jacob, R., & Steffen, M. 2005b, *A&A*, 441, 573
Schönberner, D., Jacob, R., Sandin, C., & Steffen, M. 2010, *A&A*, 523, A86